



**HAL**  
open science

## **HgCdTe-based heterostructures for terahertz photonics**

Sandra Ruffenach, Aleksandr Kadykov, V. V. Rumyantsev, Jeremie Torres,  
Dominique Coquillat, Dmytro But, Sergey S. Krishtopenko, Christophe  
Consejo, Wojciech Knap, S. Winnerl, et al.

► **To cite this version:**

Sandra Ruffenach, Aleksandr Kadykov, V. V. Rumyantsev, Jeremie Torres, Dominique Coquillat, et al.. HgCdTe-based heterostructures for terahertz photonics. *APL Materials*, 2017, 5 (3), pp.035503. 10.1063/1.4977781 . hal-01523131

**HAL Id: hal-01523131**

**<https://hal.science/hal-01523131>**

Submitted on 28 May 2021

**HAL** is a multi-disciplinary open access archive for the deposit and dissemination of scientific research documents, whether they are published or not. The documents may come from teaching and research institutions in France or abroad, or from public or private research centers.

L'archive ouverte pluridisciplinaire **HAL**, est destinée au dépôt et à la diffusion de documents scientifiques de niveau recherche, publiés ou non, émanant des établissements d'enseignement et de recherche français ou étrangers, des laboratoires publics ou privés.



Distributed under a Creative Commons Attribution 4.0 International License

# HgCdTe-based heterostructures for terahertz photonics

Cite as: APL Mater. 5, 035503 (2017); <https://doi.org/10.1063/1.4977781>

Submitted: 29 September 2016 . Accepted: 06 February 2017 . Published Online: 06 March 2017

S. Ruffenach,  A. Kadykov, V. V. Rumyantsev,  J. Torres, D. Coquillat,  D. But, S. S. Krishtopenko, C. Consejo, W. Knap,  S. Winnerl, M. Helm, M. A. Fadeev, N. N. Mikhailov,  S. A. Dvoretiskii,  V. I. Gavrilenko, S. V. Morozov, and F. Teppe

## COLLECTIONS

Paper published as part of the special topic on [Emerging Materials in Photonics](#)



View Online



Export Citation



CrossMark

## ARTICLES YOU MAY BE INTERESTED IN

[Field-effect transistors as electrically controllable nonlinear rectifiers for the characterization of terahertz pulses](#)

APL Photonics **3**, 051705 (2018); <https://doi.org/10.1063/1.5011392>

[Ultrafast graphene-based broadband THz detector](#)

Applied Physics Letters **103**, 021113 (2013); <https://doi.org/10.1063/1.4813621>

[Stimulated emission from HgCdTe quantum well heterostructures at wavelengths up to 19.5  \$\mu\text{m}\$](#)

Applied Physics Letters **111**, 192101 (2017); <https://doi.org/10.1063/1.4996966>

APL Materials

**SPECIAL TOPIC:** Materials Challenges for Nonvolatile Memory

Submit Today!

## HgCdTe-based heterostructures for terahertz photonics

S. Ruffenach,<sup>1</sup> A. Kadykov,<sup>1,2</sup> V. V. Rumyantsev,<sup>2,3</sup> J. Torres,<sup>4</sup>  
 D. Coquillat,<sup>1</sup> D. But,<sup>1</sup> S. S. Krishtopenko,<sup>1,2</sup> C. Consejo,<sup>1</sup> W. Knap,<sup>1</sup>  
 S. Winnerl,<sup>5</sup> M. Helm,<sup>5,6</sup> M. A. Fadeev,<sup>2,3</sup> N. N. Mikhailov,<sup>7,8</sup> S. A. Dvoretiskii,<sup>7</sup>  
 V. I. Gavrilenko,<sup>2,3</sup> S. V. Morozov,<sup>2,3</sup> and F. Teppe<sup>1,a</sup>

<sup>1</sup>Laboratoire Charles Coulomb, UMR CNRS 5221, University of Montpellier, Montpellier 34095, France

<sup>2</sup>Institute for Physics of Microstructures of Russian Academy of Sciences, 603950 Nizhny Novgorod, Russia

<sup>3</sup>Lobachevsky State University of Nizhny Novgorod, 603950 Nizhny Novgorod, Russia

<sup>4</sup>Institut d'Electronique et des Systèmes (IES), UMR 5214 CNRS, University of Montpellier, Montpellier 34095, France

<sup>5</sup>Institute of Ion Beam Physics and Materials Research, Helmholtz-Zentrum Dresden–Rossendorf, D–01328 Bautzner Landstraße, Dresden, Germany

<sup>6</sup>Technische Universität Dresden, D-01062 Dresden, Germany

<sup>7</sup>A. V. Rzhanov Institute of Semiconductor Physics, Siberian Branch of Russian Academy of Sciences, 630090 Novosibirsk, Russia

<sup>8</sup>Novosibirsk State University, 630090 Novosibirsk, Russia

(Received 29 September 2016; accepted 6 February 2017; published online 6 March 2017)

Due to their specific physical properties, HgCdTe-based heterostructures are expected to play an important role in terahertz photonic systems. Here, focusing on gated devices presenting inverted band ordering, we evidence an enhancement of the terahertz photoconductive response close to the charge neutrality point and at the magnetic field driven topological phase transition. We also show the ability of these heterostructures to be used as terahertz imagers. Regarding terahertz emitters, we present results on stimulated emission of HgCdTe heterostructures in their conventional semiconductor state above 30 THz, discussing the physical mechanisms involved and promising routes towards the 5–15 THz frequency domain. © 2017 Author(s). All article content, except where otherwise noted, is licensed under a Creative Commons Attribution (CC BY) license (<http://creativecommons.org/licenses/by/4.0/>). [<http://dx.doi.org/10.1063/1.4977781>]

Photonics plays a major role in information and communication technologies and their effects on human beings. The development of new photonic systems composed of efficient sources and detectors for imaging, spectroscopy, and telecommunication applications (e.g., in medicine, biology, agronomy, non-destructive testing, security) is therefore highly desirable. In this frame, the terahertz (THz) frequency range of the electromagnetic spectrum is nowadays one of the most attractive. Further advances in THz technology rely on the implementation of novel materials with original physical properties. Graphene is a promising candidate towards THz photonic systems, having already demonstrated its potential for THz lasers<sup>1</sup> and sensors.<sup>2</sup> However, HgCdTe-based heterostructures and their recently discovered fascinating physical properties<sup>3,4</sup> also attract considerable attention especially for mid-infrared (MIR) and THz photonics.

Historically, Lawson *et al.*<sup>5</sup> have demonstrated in 1959, the uncommon ability to tune the bandgap of Hg<sub>x</sub>Cd<sub>1-x</sub>Te alloys covering a wide range of wavelengths in the infrared domain paving the way towards infrared detectors<sup>6–12</sup> which are widely used nowadays. But the variable bandgap of HgCdTe structures makes them also an attractive material for THz lasers and sensors. Indeed, depending on different internal and external parameters influencing their bandgap (as Cd content, QW thickness, magnetic field, electric field, temperature, or hydrostatic pressure), these materials

<sup>a</sup>Author to whom correspondence should be addressed. Electronic mail: [Frederic.Teppe@umontpellier.fr](mailto:Frederic.Teppe@umontpellier.fr)



can be topological insulators (TIs), Dirac semimetals (DSs), or conventional narrow-gap semiconductors.<sup>13,14</sup> These different phases of matter and their transitions could be used in photonic systems to achieve high THz performances and low power consumption. For instance, in the semiconductor state, HgCdTe-based lasers could overcome the intrinsic limitations of III-V based lasers due to lattice absorption in GaAs and InP.<sup>15</sup> HgCdTe based interband lasers may therefore be used in the inaccessible 5–15 THz frequency range, since optical phonon frequencies are low enough to obtain emission below 15 THz.<sup>16</sup> In the DS state, high mobility of massless carriers is expected. Besides the evident potential for high-speed analog electronics, high electron mobility induces resonant plasma modes at THz frequencies. Moreover, the existence of a charge neutrality point (CNP) in these materials leads to a high amplitude of THz photoconductive signal. Therefore, DSs may exhibit resonant and tunable plasma modes and high THz sensitivity. In the TI regime (materials with inverted band ordering), because their charge carriers are also massless and moreover protected from backscattering by the intrinsic topology of the material band structure, HgCdTe heterostructures might be ideal to realize sensitive and low-consumption THz plasma wave detectors.

In this paper, we will investigate HgCdTe-based heterostructures as promising candidates towards THz photonic applications. The first section of the paper is devoted to the physical characterization of THz detectors and their use for practical applications as room-temperature imagers. The second section explores the possible extension of HgCdTe-based MIR emitters to THz frequencies.

In 2006, Bernevig *et al.*<sup>3</sup> predicted a topological insulator state in HgTe/Hg<sub>1-x</sub>Cd<sub>x</sub>Te quantum wells (QWs), later experimentally observed<sup>4</sup>, opening new perspectives for this II-VI material. If the HgTe QW is thinner than the critical value  $d_c = 6.3$  nm, the heterostructure behaves as a conventional semiconductor. However, in HgTe QWs wider than  $d_c$ , the E1 subband falls below the H1 subband exhibiting an inverted band ordering. The inversion between E1 and H1 subbands leads to the formation of a 2D TI state with spin-polarized helical states at the sample edges. At critical QW thickness  $d_c$ , a low-energy band structure mimics a single valley Dirac cone at the  $\Gamma$  point. This gave rise to numeral studies on the specific physical properties of these structures. For instance, focusing on photonic applications, the demonstration of the room temperature Faraday effect<sup>17</sup> opens the way towards phase modulators in the THz range, while regarding THz sensors,<sup>18,19</sup> giant photocurrent induced by THz radiation has been measured in a HgTe-based Dirac fermion system.<sup>20</sup>

The efficiency of THz photoconductive (PC) detection based on plasma wave resonant<sup>21</sup> or non-resonant<sup>22</sup> mechanisms in 2D electron gas have been experienced since more than 10 years in many materials. Elementary excitations are detected by measuring the photo-induced nonlinear change in the 2D gas conductivity induced by the THz incident field. The PC signal is measurable as a voltage drop  $\Delta U$  on the channels edges,<sup>23</sup> given by

$$\Delta U = \frac{U_a^2}{4} \times \left( \frac{1}{\sigma} \frac{d\sigma}{dV_s} \right), \quad (1)$$

where  $U_a$  is the amplitude of the radiation induced modulation of the source-to-gate voltage,  $\sigma$  is the overall channel conductivity, and  $V_s = V_G - V_{Th}$  is the swing voltage defined as the difference between the applied gate-voltage  $V_G$  and the value of the gate-voltage at the threshold  $V_{Th}$ .

To demonstrate the potential of HgTe-based heterostructures for THz photoconductive detection, two different device geometries have been chosen: gated-Hall bar and FET. A detailed description of those devices is given in Refs. 24 and 25, respectively. The high quality HgTe/Hg<sub>1-x</sub>Cd<sub>x</sub>Te QWs were grown by molecular beam epitaxy on a thick [013] oriented GaAs semi-insulating substrate.<sup>26,27</sup> Both structures exhibit an inverted band ordering at 4 K, with QW widths of 6.6 nm for the gated-Hall bar (close to the DS state), and 8.3 nm for the FET device (in the TI regime). THz-PC experiments were performed at 1.7 K and 4.2 K with a static magnetic field, perpendicular to the heterojunction-interface and tuneable between 0 and 16 T. The photo-induced voltage drop was measured along the xx-direction by using a lock-in detection system for the gated-Hall bar or between source and drain contacts for the FET. The metallic source and gate contacts are acting as the antenna for incident THz radiation coupling in these devices designed without an antenna.

In the gated-Hall Bar device, the gate leakage current was extremely low and the gate field effect allowed to control efficiently the carrier density and to change the carrier type from electrons to holes

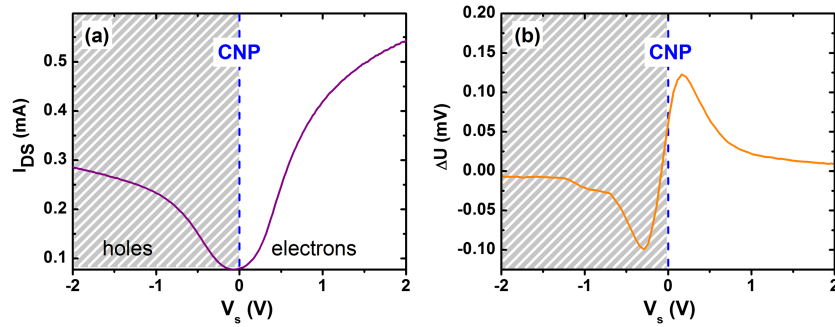


FIG. 1. Gated-Hall bar characterisation at 1.7 K and  $B = 0$  T. Dependence on swing-voltage at  $V_{\text{Drain-Source}} = 10$  mV of (a) the drain-source current and (b) the photoresponse signal ( $\Delta U$ ) under 0.17 THz illumination.

through charge neutrality point (CNP) (Fig. 1(a)). The photoconductive signal was measured under 0.17 THz radiation. In quasi-gapless materials<sup>28</sup> the photoconductivity signal exhibits a change of sign when the chemical potential below the gate crosses the charge neutrality point (CNP), exhibiting an enhanced signal in its vicinity, as shown in Fig. 1(b). This result is the first experimental demonstration of THz detection by a gated device in a topological state and paves the way towards THz topological FETs/detectors/sensors.

An alternative approach to enhance the detection sensitivity is to use the topological transitions between the different states of matter. One of the parameters inducing a phase transition between inverted band ordering and semiconductor states is the magnetic field.<sup>29</sup> In HgTe QWs exhibiting an inverted band structure, a specific dispersion of the Landau Levels (LLs) is obtained when applying a quantizing magnetic field. In this regime, the lowest LL of the conduction band contains a pure heavy hole state, when the highest LL of the valence band has a more electronic character and shifts to higher energies with the magnetic field. These two peculiar LLs, called zero-mode LLs, cross at the critical magnetic field  $B_c$ , leading to the phase transition.<sup>29</sup> Recently, Scharf *et al.*<sup>30</sup> theoretically predicted the appearance of a well-defined peak in magneto-optical conductivity at  $B_c$ . Magneto-photoconductivity experiment is a highly sensitive technique to probe mesoscopic systems with THz radiations. Elementary excitations are detected by measuring the photo-induced change of the conductivity, which monitors exactly the change of the electronic system caused by incident photons. This provides chances for exploring unique natures of excitations unable to be investigated by conventional absorption spectroscopy.

Magneto-photoconductivity measurements on the FET sensor were performed at 4.2 K by sweeping the magnetic field up to 12 T. The critical magnetic field  $B_c = 6.07$  T for the HgTe-based underlying heterostructure was calculated using a 8-band k-p Hamiltonian.<sup>25</sup> The FET photoconductivity response to THz illumination at 0.29 THz and 0.66 THz is displayed in Fig. 2(a). At  $B_c$ , a pronounced peak is clearly observed, independent of the THz radiation frequency. Magneto-absorption measurements performed on a parent sample showed no resonance at  $B_c$ , confirming that it is only observable in photoconductivity configuration. It is therefore assumed that this peak at  $B_c$  is linked to quantum phase transition driven by the magnetic field<sup>25</sup> allowing for a sensitive non-resonant detection of THz radiations in the frequency range of 0.29-0.66 THz.

Due to the magnetic field perpendicularly applied to the structure, the density of states becomes quantized. Oscillations in the photoconductivity signal take place, in a similar way than Shubnikov-de Haas (SdH) oscillations in conductivity (Fig. 2(a)). These SdH-like oscillations reflect the evolution of the density of states as a function of the magnetic field and carrier density under THz illumination. Therefore, in addition to the enhancement of the FET sensitivity, the magneto-photoconductivity technique allows to assess the inverted band structure of any gated-device.<sup>24</sup> Since this technique is almost independent of the device geometry and takes into account all the capacitances of the devices, it constitutes a powerful and versatile tool to probe the LLs of several types of 2D and 3D TI,<sup>31</sup> graphene,<sup>2</sup> or narrow-gap semiconductor based devices. Knowing that the gated-Hall bar efficiently detects THz radiation, the same magneto-photoconductivity technique was used to characterize its own physical properties. To demonstrate the validity of the photoconductivity technique to directly

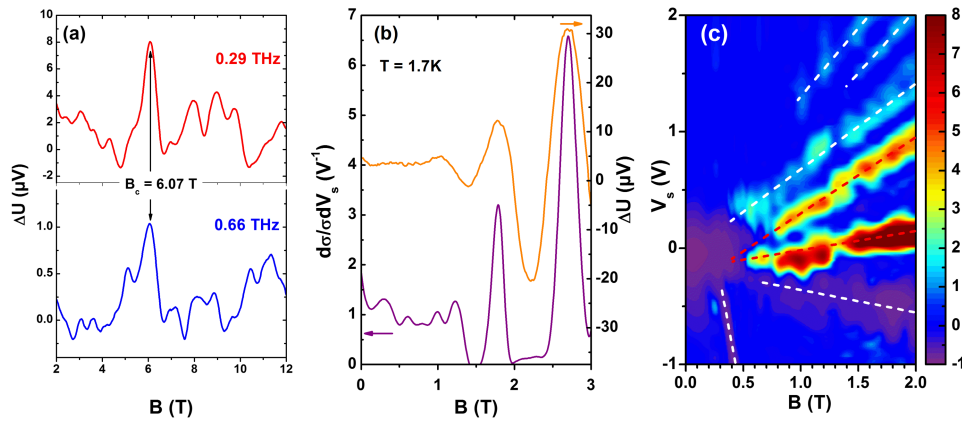


FIG. 2. THz-PC dependence on the magnetic field at low temperature. (a) FET device under THz illumination at 0.66 THz and 0.29 THz radiations, respectively (smoothed spectra). Gated-Hall bar device: (b) Comparison of PC under 0.17 THz illumination (orange) with conductivity derivative (purple) extracted from magneto-transport measurements. (c) Experimental LLs fan charts obtained by reporting the maxima of the THz-photoconductivity signal as a function of both  $V_s$  and  $B$ . Dashed lines are guide for the eyes; the red ones correspond to zero-mode LLs.

probe the LLs, we compared information resulting from magneto-transport measurements with those obtained by THz photoconductivity. For both techniques, features appear at the same magnetic fields (Fig. 2(b)), allowing a direct LL probe through the PC-technique (Fig. 2(c)). The crossing of the zero-mode LLs for the gated-Hall Bar is predicted<sup>24</sup> at  $B_c = 0.4$  T. A linear extrapolation of the zero-mode LLs in the LLs color-plot, allows to experimentally determine the value of  $B_c \approx 0.4$  T, in good agreement with theory.

One main application of HgCdTe-based THz photonics is the development of THz sensors for imaging systems.<sup>33</sup> As an example, Figure 3 shows that it is possible to use such gated devices to perform THz beam profilometry at room temperature. The same kind of device is also suitable to perform room temperature THz imaging.<sup>34</sup>

Previously, lasing in HgCdTe has been studied only in the short-wavelength part of the middle infrared range ( $2\text{--}5\ \mu\text{m}$ ).<sup>35–41</sup> Laser action at room temperature was demonstrated in QW structures at wavelengths near  $2\ \mu\text{m}$ .<sup>41</sup> In 1993, the emission wavelength of  $5.3\ \mu\text{m}$  was achieved at 45 K in diode lasers that did not exploit QWs in its design.<sup>42</sup> Soon after, III-V unipolar quantum cascade lasers (QCLs) have become the devices of choice for the  $5\text{--}15\ \mu\text{m}$  ( $60\text{--}20\ \text{THz}$ ) wavelength range, where at present QCLs can provide several watts of radiation at room temperature,<sup>43,44</sup> and THz radiation.<sup>45</sup>

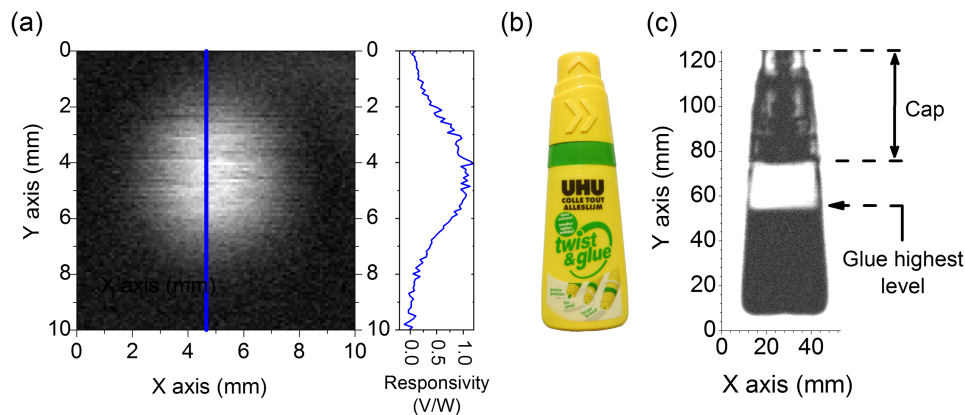


FIG. 3. (a) Image of the THz beam at 0.29 THz obtained by a FET device at room temperature. The area-normalized responsivity was estimated by taking the active area of the detector as the diffraction limited area.<sup>32</sup> (b) Visible image of a glue tube and (c) its corresponding THz image at 300 K. For the THz image, the signal-to-noise ratio is 24 dB, with 50 ms integration time.

However, the main problem of QCLs development is to further extend the radiation wavelength into the “gap” of 5–15 THz. In this spectral range, HgCdTe based interband lasers could be of use, since optical phonon frequencies in HgCdTe are low enough to get emission below 15 THz.<sup>16</sup>

The non-radiative recombination is the most important problem for the HgCdTe interband lasers in the long-wavelength region. In bulk HgCdTe, the Auger recombination rate is expected to be high, since the effective mass of a heavy hole is much higher than both the electron and light hole effective masses, which results in a low threshold energy for the Auger process. The situation is different for HgCdTe-based QWs, in which the energy spectrum in the valence band can be mirror-symmetrical to that of the conduction band. Such kind of spectra should suppress the threshold Auger processes. From this perspective, HgCdTe QWs, could be the material of choice for the THz laser. Nevertheless, according to Ref. 46 thresholdless processes can be suppressed as well, if the bandgap energy is lower than the energy distance between the edges of the lowest subbands both for holes and electrons, which is the case for the narrow gap HgTe/CdHgTe QWs. While there are a lot of works<sup>47–52</sup> and some debates concerning Auger recombination rates in a bulk material, rigorous calculations on that matter for HgCdTe QWs are very scarce in the literature. Recent experimental studies reveal weak temperature quenching of PL in QWs<sup>53,54</sup> and unexpectedly long carrier lifetimes<sup>53,55</sup> suggesting that recombination processes require further investigation.

Estimations show that narrow gap HgCdTe QWs can provide optical gain in the THz region<sup>56</sup> if the carrier density in QW is  $(1-3) \times 10^{11} \text{ cm}^{-2}$ . To achieve this carrier density via optical pumping at least  $1 \times 10^{13}$  photons are needed (QW absorption is taken as 1%). Considering a pumping source with  $\sim 2 \mu\text{m}$  pumping wavelength, beam diameter  $\sim 1 \text{ cm}$ , and typical for Q-switch laser duration pulse  $\sim 10 \text{ ns}$ , one would expect a minimal threshold excitation intensity of  $130 \text{ W/cm}^2$ . Indeed, stimulated emission (SE) can be experimentally demonstrated from narrow gap HgCdTe QWs under such pumping intensity, if a proper light confinement is guaranteed.

Figure 4(a) gives the SE spectra of the HgCdTe based structure with a thick waveguide core containing 5 QWs (see Fig. 4(b)). Each of these QWs is a 3.7 nm thick HgTe layer sandwiched between barrier layers with a Cd content of  $\sim 60\%$ . The measured carrier lifetime in the QW is  $\sim 5 \mu\text{s}$ . No mirrors were formed at the edges of the sample, yet single-pass amplification is enough to observe the intensive line of SE shifting from  $10.2 \mu\text{m}$  at 20 K to  $7.5 \mu\text{m}$  at 120 K. The threshold pumping intensity is as low as  $120 \text{ W/cm}^2$  at 20 K. Comparing it to previous work,<sup>41</sup> one can notice that with at least 3-fold increase in the SE wavelength the threshold intensity does not grow dramatically, suggesting that further improvement in the SE wavelength is feasible. The corresponding threshold current can be estimated as  $11 \text{ A/cm}^2$ . This value is at least an order of magnitude less than that of lead salt lasers operating at the same temperature and emission wavelength<sup>57,58</sup> and practically equal to the threshold current density of InAs-based interband QCL emitting near  $10.4 \mu\text{m}$  at 80 K.<sup>59</sup>

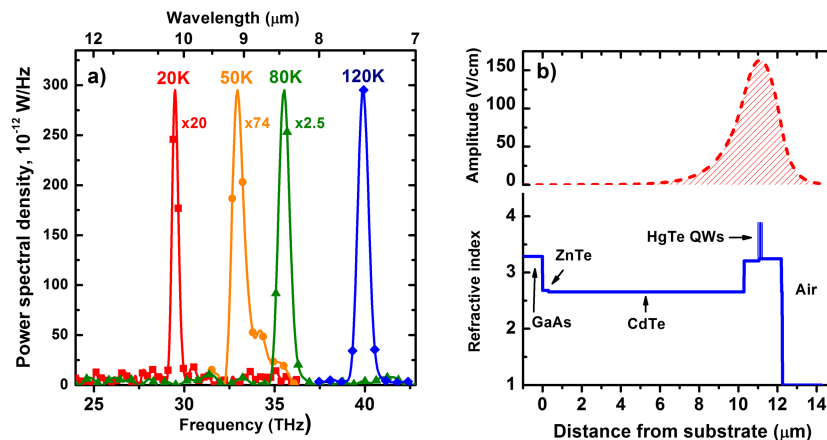


FIG. 4. (a) Spectra of stimulated emission from the structure under study at different temperatures, (b) the refractive index distribution throughout the structure and calculated mode localization for  $\lambda = 8.7 \mu\text{m}$  in the structure under study (the mode power per length unit is  $100 \text{ mW/cm}$ ).

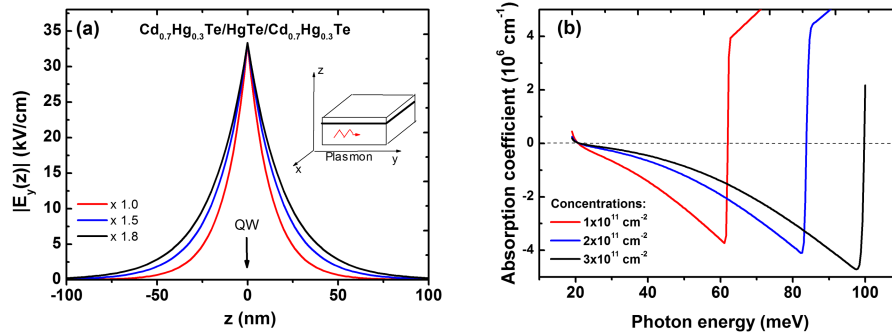


FIG. 5. Electric field distribution for  $\lambda = 35 \mu\text{m}$  (a) and calculated absorption coefficients for surface plasmon polariton (the mode power per length unit is  $100 \text{ mW/cm}$ ) (b) in HgCdTe QW with a  $20 \text{ meV}$  bandgap at different carrier densities.

In order to further increase the SE wavelength, two principal tasks should be considered. The first one is to effectively confine light in the vicinity of the active region. For wavelengths shorter than  $30 \mu\text{m}$ , thick waveguide layers can be grown in the same way as for the structure shown in Fig. 4. Below  $10 \text{ THz}$ , two-phonon absorption is important in HgCdTe and hence larger amplification coefficients are needed. A dramatic increase in gain can be achieved by employing the surface plasmon amplification in QW, like it has been proposed for graphene.<sup>60–62</sup> Fig. 5 provides the calculated electric field distribution and absorption coefficients for surface plasmon polariton in HgCdTe QW with a  $20 \text{ meV}$  bandgap at different carrier densities, based on the approach described in Ref. 60. In the regions where the absorption coefficient is negative, the amplification takes place. The electric field of a “slow” plasmon wave is very well localized near the QW (Fig. 5(a)), providing giant amplification coefficients compared to that of the photon system in the dielectric waveguide (Fig. 5(b)). However, some additional efforts are required to convert the plasmon excitation into the emitted radiation.<sup>63</sup>

Obviously, carrier lifetimes are expected to decrease for QW structures with a narrower bandgap, mainly due to Auger recombination, which is the second problem of THz lasers based on HgCdTe. The sub-nanosecond carrier lifetimes have been explored via the pump-probe measurements of a sample’s transmission using a free electron laser.<sup>64</sup> The dynamics of the sample’s transmission can thus be followed by varying the time delay of a probe pulse, i.e., the length of the optical path (Fig. 6). When the conduction and the valence band are filled with non-equilibrium carriers, the rates of the interband recombination can be estimated from the time evolution of transmission at photon energies slightly above the bandgap. There are two time scales in the transmission dynamics: a fast decay of signal is observed down to a certain value, at which it switches to a very slow decrease. The time resolved photoconductivity measurements suggest that it is of the order of  $10 \text{ ns}$ .<sup>65</sup> Estimating the

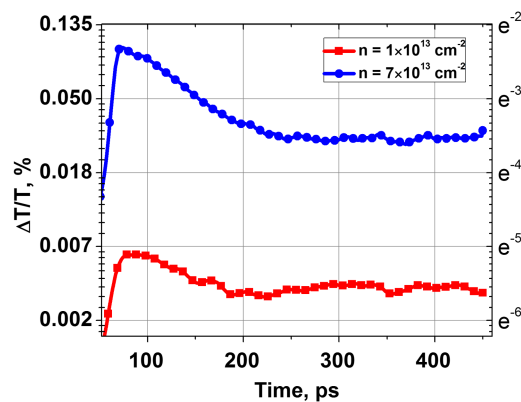


FIG. 6. The dynamics of the pump-induced transmission (divided by the transmission without pumping) for HgCdTe QW with a  $20 \text{ meV}$  bandgap at  $T = 5.5 \text{ K}$ . The transmission signal was measured via the pump-probe technique at  $\lambda = 42 \mu\text{m}$ . The legend gives the photon density in the pumping pulse.

carrier lifetime as 100 ps at the very least, one can expect a threshold pumping intensity of 10 kW/cm<sup>2</sup> for an optically pumped laser exploiting such QWs as active media. Thus, HgCdTe QWs should be able to provide amplification of radiation in the 5–15 THz range as well.

The high potential of HgCdTe heterostructures for photonic applications has been exposed focusing for both THz emitters and detectors. While for emitters the stimulated emission takes place around 30 THz, above the 5–15 THz targeted domain, the studied structures are far from being optimized yet, and further improvement in light confinement, combined with surface plasmon amplification, has been shown as promising routes. Therefore, these structures may allow to reduce the emission wavelength below 15 THz, where HgCdTe based lasers can be competitive with the main alternative technologies, in particular, III-V based QCLs. Regarding detection in the THz domain, HgCdTe-based devices exhibiting inverted band ordering at low temperature were investigated in gated-Hall Bar and FET geometries. Low temperature non-resonant photoconductivity was observed for both samples. The sensors' sensitivity was greatly enhanced close to the CNP and to the magnetic field driven topological phase transition. This high sensitivity allowed for the fine characterization of the HgCdTe heterostructure itself and the direct probing of the LLs dispersion. Finally, room temperature experiments have shown the possibility to use HgCdTe devices as THz imagers paving the way towards implementation of new THz photonic systems.

This work was supported by the CNRS through LIA TeraMIR project, by the Languedoc-Roussillon region and the MIPS department of Montpellier University via the Terahertz platform, by European cooperation through the COST action MP1204, and the Era.Net-Rus Plus project "Terasesens". F.T. and S.S.K. acknowledge the support from the Physics Department (INP) of CNRS for the post-doc prolongation program. The work was also supported by the Russian Foundation for Basic Research (Grant No. 16-32-60172). The work was done using the equipment of center "Physics and technology of micro- and nano-structures" at IPM RAS. We are grateful to P. Michel and the FELBE team for their dedicated support.

- <sup>1</sup> S. Chakraborty, O. P. Marshall, T. G. Folland, Y.-J. Kim, A. N. Grigorenko, and K. S. Novoselov, *Science* **351**, 246 (2016).
- <sup>2</sup> L. Vicarelli, M. S. Vitiello, D. Coquillat, A. Lombardo, A. C. Ferrari, W. Knap, M. Polini, V. Pellegrini, and A. Tredicucci, *Nat. Mater.* **11**, 865 (2012).
- <sup>3</sup> B. A. Bernevig, T. L. Hughes, and S.-C. Zhang, *Science* **314**, 1757 (2006).
- <sup>4</sup> M. König, S. Wiedmann, C. Brüne, A. Roth, H. Buhmann, L. W. Molenkamp, X.-L. Qi, and S.-C. Zhang, *Science* **318**, 766 (2007).
- <sup>5</sup> W. D. Lawson, S. Nielsen, E. H. Putley, and A. S. Young, *J. Phys. Chem. Solids* **9**, 325 (1959).
- <sup>6</sup> W. Lei, J. Antoszewski, and L. Faraone, *Appl. Phys. Rev.* **2**, 041303 (2015).
- <sup>7</sup> A. Rogalski, *Rep. Prog. Phys.* **68**, 2267 (2005).
- <sup>8</sup> O. Gravrand, J. Rothman, C. Cervera, N. Baier, C. Lobre, J. P. Zanatta, O. Boulade, V. Moreau, and B. Fieque, *J. Electron. Mater.* **45**, 4532 (2016).
- <sup>9</sup> C. Fulk, W. Radford, D. Buell, J. Bangs, and K. Rybnicek, *J. Electron. Mater.* **44**, 2977 (2015).
- <sup>10</sup> D. Lee, M. Carmody, E. Piquette, P. Dreiske, A. Chen, A. Yulius, D. Edwall, S. Bhargava, M. Zandian, and W. E. Tennant, *J. Electron. Mater.* **45**, 4587 (2016).
- <sup>11</sup> R. L. Strong, M. A. Kinch, and J. M. Armstrong, *J. Electron. Mater.* **42**, 3103 (2013).
- <sup>12</sup> W. Schirmacher, R. Wollrab, H. Lutz, T. Schallenberg, J. Wendler, and J. Ziegler, *J. Electron. Mater.* **43**, 2778 (2014).
- <sup>13</sup> F. Teppe, M. Marcinkiewicz, S. S. Krishtopenko, S. Ruffenach, C. Consejo, A. M. Kadykov, W. Desrat, D. But, W. Knap, J. Ludwig, S. Moon, D. Smirnov, M. Orlita, Z. Jiang, S. V. Morozov, V. I. Gavrilenko, N. N. Mikhailov, and S. A. Dvoretckii, *Nat. Commun.* **7**, 12576 (2016).
- <sup>14</sup> P. Sengupta, T. Kubis, Y. Tan, M. Povolotskyi, and G. Klimeck, *J. Appl. Phys.* **114**, 043702 (2013).
- <sup>15</sup> F. Castellano, A. Bismuto, M. I. Amanti, R. Terazzi, M. Beck, S. Blaser, A. Bächle, and J. Faist, *J. Appl. Phys.* **109**, 102407 (2011).
- <sup>16</sup> D. N. Talwar and M. Vandevyver, *J. Appl. Phys.* **56**, 1601 (1984).
- <sup>17</sup> P. Olbrich, C. Zoth, P. Vierling, K.-M. Dantscher, G. V. Budkin, S. A. Tarasenko, V. V. Bel'kov, D. A. Kozlov, Z. D. Kvon, N. N. Mikhailov, S. A. Dvoretckii, and S. D. Ganichev, *Phys. Rev. B* **87**, 235439 (2013).
- <sup>18</sup> F. Sizov, V. Zabudsky, S. Dvoretckii, V. Petryakov, A. Golenkov, K. Andreyeva, and Z. Tsybrii, *Appl. Phys. Lett.* **106**, 082104 (2015).
- <sup>19</sup> F. Gouider, G. Nachtwei, C. Brüne, H. Buhmann, Yu. B. Vasilyev, M. Salman, J. Könnemann, and P. D. Buckle, *J. Appl. Phys.* **109**, 013106 (2011).
- <sup>20</sup> A. M. Shuvaev, G. V. Astakhov, A. Pimenov, C. Brüne, H. Buhmann, and L. W. Molenkamp, *Phys. Rev. Lett.* **106**, 107404 (2011).
- <sup>21</sup> M. Dyakonov and M. Shur, *Phys. Rev. Lett.* **71**, 2465 (1993).
- <sup>22</sup> M. Sakowicz, M. B. Lifshits, O. A. Klimenko, F. Schuster, D. Coquillat, F. Teppe, and W. Knap, *J. Appl. Phys.* **110**, 054512 (2011).

- <sup>23</sup> W. Knap, M. Dyakonov, D. Coquillat, F. Teppe, N. Dyakonova, J. Łusakowski, K. Karpierz, M. Sakowicz, G. Valusis, D. Seliuta, I. Kasalynas, A. El Fatimy, Y. M. Meziani, and T. Otsuji, *J. Infrared, Millimeter, Terahertz Waves* **30**, 1319 (2009).
- <sup>24</sup> A. Kadykov, J. Torres, S. S. Krishtopenko, C. Consejo, S. Ruffenach, M. Marcinkiewicz, D. But, W. Knap, S. V. Morozov, V. I. Gavrilenko, N. N. Mikhailov, S. A. Dvoretzky, and F. Teppe, *Appl. Phys. Lett.* **108**, 262102 (2016).
- <sup>25</sup> A. M. Kadykov, F. Teppe, C. Consejo, L. Viti, M. S. Vitiello, S. S. Krishtopenko, S. Ruffenach, S. V. Morozov, M. Marcinkiewicz, W. Desrat, N. Dyakonova, W. Knap, V. I. Gavrilenko, N. N. Mikhailov, and S. A. Dvoretzky, *Appl. Phys. Lett.* **107**, 152101 (2015).
- <sup>26</sup> D. A. Kozlov, Z. D. Kvon, N. N. Mikhailov, and S. A. Dvoretzky, *JETP Lett.* **96**, 730 (2013).
- <sup>27</sup> S. Dvoretzky, N. Mikhailov, Y. Sidorov, V. Shvets, S. Danilov, B. Wittman, and S. Ganichev, *J. Electron. Mater.* **39**, 918 (2010).
- <sup>28</sup> A. K. Geim and K. S. Novoselov, *Nat. Mater.* **6**, 183 (2007).
- <sup>29</sup> M. Zholudev, F. Teppe, M. Orlita, C. Consejo, J. Torres, N. Dyakonova, M. Czapkiewicz, J. Wröbel, G. Grabecki, N. Mikhailov, S. Dvoretzky, A. Ikonnikov, K. Spirin, V. Aleshkin, V. Gavrilenko, and W. Knap, *Phys. Rev. B* **86**, 205420 (2012).
- <sup>30</sup> B. Scharf, A. Matos-Abiague, I. Zutic', and J. Fabian, *Phys. Rev. B* **91**, 235433 (2015).
- <sup>31</sup> D. A. Kozlov, D. Bauer, J. Ziegler, R. Fisher, M. L. Savchenko, Z. D. Kvon, N. N. Mikhailov, S. A. Dvoretzky, and D. Weiss, *Phys. Rev. Lett.* **116**, 166802 (2016).
- <sup>32</sup> R. Tauk, F. Teppe, S. Boubanga, D. Coquillat, W. Knap, Y. M. Meziani, C. Gallon, F. Boeuf, T. Skotnicki, C. Fenouillet-Beranger, D. K. Maude, S. Romyantsev, and M. S. Shur, *Appl. Phys. Lett.* **97**, 052108 (2010).
- <sup>33</sup> F. F. Sizov, V. V. Zabudsky, A. G. Golenkov, and A. Shevchik-Sheker, *Opt. Eng.* **52**, 033203 (2013).
- <sup>34</sup> F. Schuster, D. Coquillat, H. Videlier, M. Sakowicz, F. Teppe, L. Dussopt, B. Giffard, T. Skotnicki, and W. Knap, *Opt. Express* **19**, 7827 (2011).
- <sup>35</sup> A. A. Andronov, Yu. N. Nozdrin, A. V. Okomel'kov, A. A. Babenko, V. S. Varavin, D. G. Ikusov, and R. N. Smirnov, *Semiconductors* **42**, 179 (2008).
- <sup>36</sup> J. Bonnet-Gamard, J. Bleuse, N. Magnea, and J. L. Pautrat, *J. Appl. Phys.* **78**, 6908 (1995).
- <sup>37</sup> E. Hadji, J. Bleuse, N. Magnea, and J. L. Pautrat, *Appl. Phys. Lett.* **67**, 2591 (1995).
- <sup>38</sup> E. Hadji, J. Bleuse, N. Magnea, and J. L. Pautrat, *Appl. Phys. Lett.* **68**, 2480 (1996).
- <sup>39</sup> A. Ravid, G. Cinader, and A. Zussman, *J. Appl. Phys.* **74**, 15 (1993).
- <sup>40</sup> C. Roux, E. Hadji, and J. L. Pautrat, *Appl. Phys. Lett.* **75**, 3763 (1999).
- <sup>41</sup> J. Bleuse, J. Bonnet-Gamard, G. Mula, N. Magnea, and J. L. Pautrat, *J. Cryst. Growth* **197**, 529 (1999).
- <sup>42</sup> J. M. Arias, M. Zandian, R. Zucca, and J. Singh, *Semicond. Sci. Technol.* **8**, S255 (1993).
- <sup>43</sup> N. Bandyopadhyay, Y. Bai, S. Slivken, and M. Razeghi, *Appl. Phys. Lett.* **105**, 071106 (2014).
- <sup>44</sup> M. S. Vitiello, G. Scalari, B. Williams, and P. De Natale, *Opt. Express* **23**, 5167 (2015).
- <sup>45</sup> B. S. Williams, *Nat. Photon* **1**, 517 (2007).
- <sup>46</sup> A. S. Polkovnikov and G. G. Zegrya, *Phys. Rev. B* **58**, 4039 (1998).
- <sup>47</sup> S. Krishnamurthy, M. A. Berding, and Z. G. Yu, *J. Electron. Mater.* **35**, 1369 (2006).
- <sup>48</sup> Y. Chang, C. H. Grein, J. Zhao, C. R. Becker, M. E. Flatte, P. K. Liao, F. Aqariden, and S. Sivananthan, *Appl. Phys. Lett.* **93**, 192111 (2008).
- <sup>49</sup> D. Donetsky, G. Belenky, S. Svensson, and S. Suchalkin, *Appl. Phys. Lett.* **97**, 052108 (2010).
- <sup>50</sup> K. Jóźwikowski, M. Kopytko, and A. Rogalski, *J. Appl. Phys.* **112**, 033718 (2012).
- <sup>51</sup> H. Wen, B. Pinkie, and E. Bellotti, *J. Appl. Phys.* **118**, 015702 (2015).
- <sup>52</sup> B. L. Gel'mont, *Sov. Phys. JETP* **48**, 268 (1978).
- <sup>53</sup> S. V. Morozov, V. V. Romyantsev, A. V. Antonov, A. M. Kadykov, K. V. Maremyanin, K. E. Kudryavtsev, N. N. Mikhailov, S. A. Dvoretzky, and V. I. Gavrilenko, *Appl. Phys. Lett.* **105**, 022102 (2014).
- <sup>54</sup> I. I. Izhnin, A. I. Izhnin, K. D. Mynbaev, N. L. Bazhenov, A. V. Shilyaev, N. N. Mikhailov, V. S. Varavin, S. A. Dvoretzky, O. I. Fitsych, and A. V. Voitsekhovskiy, *Opto-Electron. Rev.* **21**, 390 (2013).
- <sup>55</sup> S. V. Morozov, V. V. Romyantsev, A. M. Kadykov, A. A. Dubinov, A. V. Antonov, K. E. Kudryavtsev, D. I. Kuritsin, N. N. Mikhailov, S. A. Dvoretzky, F. Teppe, and V. I. Gavrilenko, *J. Phys.: Conf. Ser.* **647**, 012008 (2015).
- <sup>56</sup> S. V. Morozov, M. S. Joludev, A. V. Antonov, V. V. Romyantsev, V. I. Gavrilenko, V. Ya Aleshkin, A. A. Dubinov, N. N. Mikhailov, S. A. Dvoretzky, O. Drachenko, S. Winnerl, H. Schneider, and M. Helm, *Semiconductors* **46**, 1362 (2012).
- <sup>57</sup> A. P. Shotov, *AIP Conf. Proc.* **240**, 87 (1991).
- <sup>58</sup> K. V. Maremyanin, A. V. Ikonnikov, A. V. Antonov, V. V. Romyantsev, S. V. Morozov, L. S. Bovkun, K. R. Umbetalieva, E. G. Chizhevskiy, I. I. Zasavitskiy, and V. I. Gavrilenko, *Semiconductors* **49**, 1623 (2015).
- <sup>59</sup> Z. Tian, L. Li, H. Ye, R. Q. Yang, T. D. Mishima, M. B. Santos, and M. B. Johnson, *Electron. Lett.* **48**, 113 (2012).
- <sup>60</sup> A. A. Dubinov, V. Ya Aleshkin, V. Mitin, T. Otsuji, and V. Ryzhii, *J. Phys.: Condens. Matter* **23**, 145302 (2011).
- <sup>61</sup> T. Otsuji, T. Watanabe, S. Boubanga Tombet, Y. Yabe, A. Satou, A. A. Dubinov, V. Y. Aleshkin, V. Mitin, and V. Ryzhii, *SPIE Newsroom* (2014).
- <sup>62</sup> F. Rana, *IEEE Trans. Nanotechnol.* **7**, 91 (2008).
- <sup>63</sup> V. V. Popov, O. V. Polischuk, A. R. Davoyan, V. Ryzhii, T. Otsuji, and M. S. Shur, *Phys. Rev. B* **86**, 195437 (2012).
- <sup>64</sup> S. Winnerl, M. Orlita, P. Plochocka, P. Kossacki, M. Potemski, T. Winzer, E. Malic, A. Knorr, M. Sprinkle, C. Berger, W. A. de Heer, H. Schneider, and M. Helm, *Phys. Rev. Lett.* **107**, 237401 (2011).
- <sup>65</sup> V. V. Romyantsev, A. V. Ikonnikov, A. V. Antonov, S. V. Morozov, M. S. Zholudev, K. E. Spirin, V. I. Gavrilenko, S. A. Dvoretzky, and N. N. Mikhailov, *Semiconductors* **47**(11), 1438 (2013).